

Study of the Strong Coupling Constant Using $W + \text{Jet}$ Processes

S. Abachi,¹² B. Abbott,³⁴ M. Abolins,²³ B. S. Acharya,⁴² I. Adam,¹⁰ D. L. Adams,³⁵ M. Adams,¹⁵ S. Ahn,¹² H. Aihara,²⁰ J. Alitti,³⁸ G. Álvarez,¹⁶ G. A. Alves,⁸ E. Amidi,²⁷ N. Amos,²² E. W. Anderson,¹⁷ S. H. Aronson,³ R. Astur,⁴⁰ R. E. Avery,²⁹ A. Baden,²¹ V. Balamurali,³⁰ J. Balderston,¹⁴ B. Baldin,¹² J. Bantly,⁴ J. F. Bartlett,¹² K. Bazizi,³⁷ J. Bendich,²⁰ S. B. Beri,³² I. Bertram,³⁵ V. A. Bezzubov,³³ P. C. Bhat,¹² V. Bhatnagar,³² M. Bhattacharjee,¹¹ A. Bischoff,⁷ N. Biswas,³⁰ G. Blazey,¹² S. Blessing,¹³ P. Bloom,⁵ A. Boehnlein,¹² N. I. Bojko,³³ F. Borchering,¹² J. Borders,³⁷ C. Boswell,⁷ A. Brandt,¹² R. Brock,²³ A. Bross,¹² D. Buchholz,²⁹ V. S. Burtovoi,³³ J. M. Butler,¹² W. Carvalho,⁸ D. Casey,³⁷ H. Castilla-Valdez,⁹ D. Chakraborty,⁴⁰ S.-M. Chang,²⁷ S. V. Chekulaev,³³ L.-P. Chen,²⁰ W. Chen,⁴⁰ L. Chevalier,³⁸ S. Chopra,³² B. C. Choudhary,⁷ J. H. Christenson,¹² M. Chung,¹⁵ D. Claes,⁴⁰ A. R. Clark,²⁰ W. G. Cobau,²¹ J. Cochran,⁷ W. E. Cooper,¹² C. Cretsinger,³⁷ D. Cullen-Vidal,⁴ M. A. C. Cummings,¹⁴ D. Cutts,⁴ O. I. Dahl,²⁰ K. De,⁴³ M. Demarteau,¹² R. Demina,²⁷ K. Denisenko,¹² N. Denisenko,¹² D. Denisov,¹² S. P. Denisov,³³ W. Dharmaratna,¹³ H. T. Diehl,¹² M. Diesburg,¹² G. Di Loreto,²³ R. Dixon,¹² P. Draper,⁴³ J. Drinkard,⁶ Y. Ducros,³⁸ S. R. Dugad,⁴² S. Durston-Johnson,³⁷ D. Edmunds,²³ J. Ellison,⁷ V. D. Elvira,^{12,*} R. Engelmann,⁴⁰ S. Eno,²¹ G. Eppley,³⁵ P. Ermolov,²⁴ O. V. Eroshin,³³ V. N. Evdokimov,³³ S. Fahey,²³ T. Fahland,⁴ M. Fatyga,³ M. K. Fatyga,³⁷ J. Featherly,³ S. Feher,⁴⁰ D. Fein,² T. Ferbel,³⁷ G. Finocchiaro,⁴⁰ H. E. Fisk,¹² Y. Fisyak,⁵ E. Flattum,²³ G. E. Forden,² M. Fortner,²⁸ K. C. Frame,²³ P. Franzini,¹⁰ S. Fuess,¹² E. Gallas,⁴³ A. N. Galyaev,³³ S. G. Gao,^{12,†} T. L. Geld,²³ R. J. Genik II,²³ K. Genser,¹² C. E. Gerber,^{12,‡} B. Gibbard,³ V. Glebov,³ S. Glenn,⁵ B. Gobbi,²⁹ M. Goforth,¹³ A. Goldschmidt,²⁰ B. Gómez,¹ P. I. Goncharov,³³ J. L. González Solís,⁹ H. Gordon,³ L. T. Goss,⁴⁴ N. Graf,³ P. D. Grannis,⁴⁰ D. R. Green,¹² J. Green,²⁸ H. Greenlee,¹² G. Griffin,⁶ N. Grossman,¹² P. Grudberg,²⁰ S. Grünendahl,³⁷ W. X. Gu,^{12,†} G. Guglielmo,³¹ J. A. Guida,⁴⁰ J. M. Guida,³ W. Guryn,³ S. N. Gurzhev,³³ P. Gutierrez,³¹ Y. E. Gutnikov,³³ N. J. Hadley,²¹ H. Haggerty,¹² S. Hagopian,¹³ V. Hagopian,¹³ K. S. Hahn,³⁷ R. E. Hall,⁶ S. Hansen,¹² R. Hatcher,²³ J. M. Hauptman,¹⁷ D. Hedin,²⁸ A. P. Heinson,⁷ U. Heintz,¹² R. Hernández-Montoya,⁹ T. Heuring,¹³ R. Hirosky,¹³ J. D. Hobbs,¹² B. Hoeneisen,^{1,§} J. S. Hoftun,⁴ F. Hsieh,²² Tao Hu,^{12,†} Ting Hu,⁴⁰ Tong Hu,¹⁶ T. Huehn,⁷ S. Igarashi,¹² A. S. Ito,¹² E. James,² J. Jaques,³⁰ S. A. Jerger,²³ J. Z.-Y. Jiang,⁴⁰ T. Joffe-Minor,²⁹ H. Johari,²⁷ K. Johns,² M. Johnson,¹² H. Johnstad,⁴¹ A. Jonckheere,¹² M. Jones,¹⁴ H. Jöstlein,¹² S. Y. Jun,²⁹ C. K. Jung,⁴⁰ S. Kahn,³ G. Kalbfleisch,³¹ J. S. Kang,¹⁸ R. Kehoe,³⁰ M. L. Kelly,³⁰ A. Kernan,⁷ L. Kerth,²⁰ C. L. Kim,¹⁸ S. K. Kim,³⁹ A. Klatchko,¹³ B. Klima,¹² B. I. Klochkov,³³ C. Klopfenstein,⁵ V. I. Klyukhin,³³ V. I. Kochetkov,³³ J. M. Kohli,³² D. Koltick,³⁴ A. V. Kostritskiy,³³ J. Kotcher,³ J. Kourlas,²⁶ A. V. Kozelov,³⁸ E. A. Kozlovski,³³ M. R. Krishnaswamy,⁴² S. Krzywdzinski,¹² S. Kunori,²¹ S. Lami,⁴⁰ G. Landsberg,¹² J.-F. Lebrat,³⁸ A. Leflat,²⁴ H. Li,⁴⁰ J. Li,⁴³ Y. K. Li,²⁹ Q. Z. Li-Demarteau,¹² J. G. R. Lima,³⁶ D. Lincoln,²² S. L. Linn,¹³ J. Linnemann,²³ R. Lipton,¹² Y. C. Liu,²⁹ F. Lobkowicz,³⁷ S. C. Loken,²⁰ S. Lökös,⁴⁰ L. Lueking,¹² A. L. Lyon,²¹ A. K. A. Maciel,⁸ R. J. Madaras,²⁰ R. Madden,¹³ I. V. Mandrichenko,³³ Ph. Mangeot,³⁸ S. Mani,⁵ B. Mansoulié,³⁸ H. S. Mao,^{12,†} S. Margulies,¹⁵ R. Markeloff,²⁸ L. Markosky,² T. Marshall,¹⁶ M. I. Martin,¹² M. Marx,⁴⁰ B. May,²⁹ A. A. Mayorov,³³ R. McCarthy,⁴⁰ T. McKibben,¹⁵ J. McKinley,²³ T. McMahon,³¹ H. L. Melanson,¹² J. R. T. de Mello Neto,³⁶ K. W. Merritt,¹² H. Miettinen,³⁵ A. Milder,² A. Mincer,²⁶ J. M. de Miranda,⁸ C. S. Mishra,¹² M. Mohammadi-Baarmand,⁴⁰ N. Mokhov,¹² N. K. Mondal,⁴² H. E. Montgomery,¹² P. Mooney,¹ M. Mudan,²⁶ C. Murphy,¹⁶ C. T. Murphy,¹² F. Nang,⁴ M. Narain,¹² V. S. Narasimham,⁴² A. Narayanan,² H. A. Neal,²² J. P. Negret,¹ E. Neis,²² P. Nemethy,²⁶ D. Nešić,⁴ M. Nicola,⁸ D. Norman,⁴⁴ L. Oesch,²² V. Oguri,³⁶ E. Oltman,²⁰ N. Oshima,¹² D. Owen,²³ P. Padley,³⁵ M. Pang,¹⁷ A. Para,¹² C. H. Park,¹² Y. M. Park,¹⁹ R. Partridge,⁴ N. Parua,⁴² M. Paterno,³⁷ J. Perkins,⁴³ A. Peryshkin,¹² M. Peters,¹⁴ H. Piekarczyk,¹³ Y. Pischalnikov,³⁴ A. Pluquet,³⁸ V. M. Podstavkov,³³ B. G. Pope,²³ H. B. Prosper,¹³ S. Protopopescu,³ D. Pušeljčić,²⁰ J. Qian,²² P. Z. Quintas,¹² R. Raja,¹² S. Rajagopalan,⁴⁰ O. Ramirez,¹⁵ M. V. S. Rao,⁴² P. A. Rapidis,¹² L. Rasmussen,⁴⁰ A. L. Read,¹² S. Reucroft,²⁷ M. Rijssenbeek,⁴⁰ T. Rockwell,²³ N. A. Roe,²⁰ P. Rubinov,⁴⁰ R. Ruchti,³⁰ S. Rusin,²⁴ J. Rutherford,² A. Santoro,⁸ L. Sawyer,⁴³ R. D. Schamberger,⁴⁰ H. Schellman,²⁹ J. Sculli,²⁶ E. Shabalina,²⁴ C. Shaffer,¹³ H. C. Shankar,⁴² Y. Y. Shao,^{12,†} R. K. Shivpuri,¹¹ M. Shupe,² J. B. Singh,³² V. Sirotenko,²⁸ W. Smart,¹² A. Smith,² R. P. Smith,¹² R. S. Snihur,²⁹ G. R. Snow,²⁵ S. Snyder,⁴⁰ J. Solomon,¹⁵ P. M. Sood,³² M. Sosebee,⁴³ M. Souza,⁸ A. L. Spadafora,²⁰ R. W. Stephens,⁴³ M. L. Stevenson,²⁰ D. Stewart,²² D. A. Stoianova,³³ D. Stoker,⁶ K. Streets,²⁶ M. Strovink,²⁰ A. Sznajder,⁸ A. Taketani,¹² P. Tamburello,²¹ J. Tarazi,⁶ M. Tartaglia,¹² T. L. Taylor,²⁹ J. Teiger,³⁸ J. Thompson,²¹ T. G. Trippe,²⁰ P. M. Tuts,¹⁰ N. Varelas,²³ E. W. Varnes,²⁰ P. R. G. Virador,²⁰ D. Vititoe,² A. A. Volkov,³³

A. P. Vorobiev,³³ H. D. Wahl,¹³ G. Wang,¹³ J. Wang,^{12,†} J. Warchol,³⁰ M. Wayne,³⁰ H. Weerts,²³ F. Wen,¹³
 W. A. Wenzel,²⁰ A. White,⁴³ J. T. White,⁴⁴ J. A. Wightman,¹⁷ J. Wilcox,²⁷ S. Willis,²⁸ S. J. Wimpenny,⁷
 J. V. D. Wirjawan,⁴⁴ J. Womersley,¹² E. Won,³⁷ D. R. Wood,¹² H. Xu,⁴ R. Yamada,¹² P. Yamin,³ C. Yanagisawa,⁴⁰
 J. Yang,²⁶ T. Yasuda,²⁷ C. Yoshikawa,¹⁴ S. Youssef,¹³ J. Yu,³⁷ Y. Yu,³⁹ D. H. Zhang,^{12,†} Y. Zhang,^{12,†} Q. Zhu,²⁶
 Z. H. Zhu,³⁷ D. Zieminska,¹⁶ A. Zieminski,¹⁶ and A. Zylberstejn³⁸

(D0 Collaboration)

¹Universidad de los Andes, Bogotá, Colombia

²University of Arizona, Tucson, Arizona 85721

³Brookhaven National Laboratory, Upton, New York 11973

⁴Brown University, Providence, Rhode Island 02912

⁵University of California, Davis, California 95616

⁶University of California, Irvine, California 92717

⁷University of California, Riverside, California 92521

⁸LAFEX, Centro Brasileiro de Pesquisas Físicas, Rio de Janeiro, Brazil

⁹Centro de Investigación y de Estudios Avanzados, Mexico City, Mexico

¹⁰Columbia University, New York, New York 10027

¹¹Delhi University, Delhi, India 110007

¹²Fermi National Accelerator Laboratory, Batavia, Illinois 60510

¹³Florida State University, Tallahassee, Florida 32306

¹⁴University of Hawaii, Honolulu, Hawaii 96822

¹⁵University of Illinois at Chicago, Chicago, Illinois 60607

¹⁶Indiana University, Bloomington, Indiana 47405

¹⁷Iowa State University, Ames, Iowa 50011

¹⁸Korea University, Seoul, Korea

¹⁹Kyungshung University, Pusan, Korea

²⁰Lawrence Berkeley Laboratory and University of California, Berkeley, California 94720

²¹University of Maryland, College Park, Maryland 20742

²²University of Michigan, Ann Arbor, Michigan 48109

²³Michigan State University, East Lansing, Michigan 48824

²⁴Moscow State University, Moscow, Russia

²⁵University of Nebraska, Lincoln, Nebraska 68588

²⁶New York University, New York, New York 10003

²⁷Northeastern University, Boston, Massachusetts 02115

²⁸Northern Illinois University, DeKalb, Illinois 60115

²⁹Northwestern University, Evanston, Illinois 60208

³⁰University of Notre Dame, Notre Dame, Indiana 46556

³¹University of Oklahoma, Norman, Oklahoma 73109

³²University of Panjab, Chandigarh 16-00-14, India

³³Institute for High Energy Physics, 142-284 Protvino, Russia

³⁴Purdue University, West Lafayette, Indiana 47907

³⁵Rice University, Houston, Texas 77251

³⁶Universidade Estadual do Rio de Janeiro, Rio de Janeiro, Brazil

³⁷University of Rochester, Rochester, New York 14627

³⁸Commissariat à l'Énergie Atomique, DAPNIA/Service de Physique des Particules, Centre d'Études de Saclay, Saclay, France

³⁹Seoul National University, Seoul, Korea

⁴⁰State University of New York, Stony Brook, New York 11794

⁴¹Superconducting Super Collider Laboratory, Dallas, Texas 75237

⁴²Tata Institute of Fundamental Research, Colaba, Bombay 400005, India

⁴³University of Texas, Arlington, Texas 76019

⁴⁴Texas A&M University, College Station, Texas 77843

(Received 17 April 1995; revised manuscript received 12 July 1995)

The ratio of the number of $W + 1$ jet to $W + 0$ jet events is measured with the D0 detector using data from the 1992–93 Tevatron Collider run. For the $W \rightarrow e\nu$ channel with a minimum jet E_T cutoff of 25 GeV, the experimental ratio is $0.065 \pm 0.003(\text{stat}) \pm 0.007(\text{sys})$. Next-to-leading order QCD predictions for various parton distributions agree well with each other and are all over 1 standard deviation below the measurement. Varying the strong coupling constant α_s , in both the parton distributions and the partonic cross sections simultaneously does not remove this discrepancy.

PACS numbers: 12.38.Qk, 13.85.Qk, 13.87.Ce

The running coupling constant α_s is a fundamental expansion parameter which sets the strength of all strong interactions. Of particular interest in the current study is the fact that the probability of producing jets in association with a W boson is dependent upon the value of α_s . We report here the results of an attempt to extract the value of α_s from an examination of the ratio \mathcal{R} of $W + 1$ jet to $W + 0$ jet cross sections. A similar technique, based on tree-level calculations, has been used by the UA2 [1] and UA1 experiments [2].

In leading-order (LO) QCD, \mathcal{R} is proportional to α_s . However, the cross sections computed at LO suffer from relatively large normalization uncertainties due to the lack of higher order corrections. Recent next-to-leading order (NLO) predictions [3] of the $W + 0$ jet and $W + 1$ jet cross sections show significantly reduced μ_R dependence and differ from LO predictions by about 10% for μ_R equal to the W mass (M_W) [4].

We present an experimental measurement of the ratio, $\mathcal{R}_{\text{meas}}$, using the D0 detector at the Fermilab Tevatron $\bar{p}p$ Collider at $\sqrt{s} = 1.8$ TeV. We utilize 9770 $W \rightarrow e\nu$ candidates collected during the 1992–93 collider run. The experimental result $\mathcal{R}_{\text{meas}}$ is compared with NLO theoretical predictions [5].

The D0 detector is described in detail elsewhere [6]. The detector elements relevant to this analysis are the tracking system and the uranium liquid-argon sampling calorimeter. The tracking system, which has no magnetic field, covers a range of pseudorapidity η [7] from -3.0 to 3.0 . The calorimeter's homogeneous response and hermetic coverage out to $|\eta| \sim 4$ provide excellent measurement of electron and jet energies, as well as missing transverse energy (\cancel{E}_T), over the full azimuth (ϕ). The calorimeter is finely segmented in both the longitudinal and transverse directions, giving enhanced electron identification. The electron energy resolution is $15\%/\sqrt{E(\text{GeV})}$ and the jet transverse energy (E_T) resolution is $\sim 80\%/\sqrt{E_T(\text{GeV})}$.

For this analysis, we use a hardware trigger which requires events with a minimum E_T of 10 GeV in an electromagnetic (EM) calorimeter trigger tower of size 0.2×0.2 in η - ϕ space, covering $|\eta| < 3.2$. Events satisfying the hardware trigger are subjected to a software trigger which requires the event to have $\cancel{E}_T > 20$ GeV and to have an electron candidate which has transverse energy (E_T^e) greater than 20 GeV and passes preliminary shower shape and isolation cuts.

The off-line selection of the $W \rightarrow e\nu$ event sample requires $\cancel{E}_T > 25$ GeV and an electron with $E_T^e > 25$ GeV which satisfies three electron quality criteria. The first involves the isolation fraction which is defined as $f_{\text{iso}} = [E(0.4) - E_{\text{EM}}(0.2)]/E_{\text{EM}}(0.2)$, where $E(0.4)$ is the total energy within a cone of radius 0.4 [$\Delta R \equiv \sqrt{(\Delta\eta)^2 + (\Delta\phi)^2}$] centered around the electron, and $E_{\text{EM}}(0.2)$ is the electromagnetic energy within $\Delta R = 0.2$. A cut of $f_{\text{iso}} < 0.15$ is imposed to require that the elec-

tron is isolated from other sources of energy in the event. The second criterion is that the calorimeter energy deposition of the electron has a matching charged track. Finally, a cut is imposed on the χ^2 value of the energy cluster to ensure that its shape is consistent with that of an electron. This value of χ^2 is computed using a 41 dimensional energy covariance matrix [8], which has the mean cell energy depositions of a reference electron shower as its elements, preserving their correlations.

Given the nature of $\mathcal{R}_{\text{meas}}$, it is advantageous, in minimizing systematic uncertainties, to have the electron selection efficiency be the same for events with and without an associated jet. The electron selection criteria applied to the $W \rightarrow e\nu$ candidates preclude the use of this data sample for estimating the selection efficiency because the only electron in the event is already subjected to the selection criteria. Therefore, we use $Z(\rightarrow e^+e^-) + 0$ jet and $Z + 1$ jet candidates from actual data, where only one of the two electrons is required to pass the selection criteria. The electron selection efficiency is then measured by imposing the selection criteria on the other electron. From this study, the electron selection efficiency is found to be the same for these jet multiplicities (0 jet and 1 jet) to within 2%.

Jets in the events are identified with a fixed cone algorithm using a radius $\Delta R = 0.7$. The jet reconstruction efficiency is found to be better than 99% for jets with $E_T > 20$ GeV, based on a Monte Carlo study [9]. The jet E_T is corrected for the calorimeter response, out-of-cone showering, and the underlying event contribution. The jet energy scale correction [10] is obtained by using events with photon + jet final states. In these events, the photon candidate is taken to balance the remaining partons in the event kinematically. The components of the transverse momentum imbalance due to the mismeasurement in hadronic jet energy are then corrected using the \cancel{E}_T projection on the photon candidate axis. The typical size of the correction is $(16 \pm 5)\%$ at 25 GeV and $(24 \pm 5)\%$ at 100 GeV. The jets are required to have a minimum transverse energy (E_T^{min}) of 25 GeV. Before background subtraction, 5736 $W + 0$ jet events have the electron in the central region ($|\eta_e| < 1.2$) and 3083 events have the electron in the forward region ($|\eta_e| > 1.2$). The corresponding numbers of events with one jet are 511 and 284 events, respectively.

The largest background to the $W \rightarrow e\nu$ production comes from multijet processes. A jet from a multijet event may pass all electron selection criteria due to fluctuations in fragmentation. Significant \cancel{E}_T may also be associated with multijet events due to shower fluctuations or calorimeter imperfections. Occasionally a multijet event has both significant \cancel{E}_T and a jet imitating an electron and thereby simulates a $W \rightarrow e\nu$ event.

The fractional background from multijet events is estimated using the \cancel{E}_T distributions from data for events that pass an inclusive electron trigger ($E_T^e > 20$ GeV).

The sample is separated into two subsets. The first subset consists of events failing all three of the electron quality criteria (f_{iso} , track matching, and χ^2). Real electrons from W decays contribute negligibly to this subset. The second subset consists of events which pass the three electron quality criteria. This subset includes both backgrounds from multijet events and real W events. The histogram in Fig. 1 represents the \cancel{E}_T distribution of events with electrons satisfying the three electron quality criteria (signal + background) and the solid circles represent the other subset (background). A clear separation between signal and background above $\cancel{E}_T = 20$ GeV is evident because the \cancel{E}_T due to the neutrino in W decay peaks near 40 GeV and far less \cancel{E}_T is expected in true multijet events. The shapes of the two distributions agree well for $\cancel{E}_T < 15$ GeV. The background distribution for $\cancel{E}_T > 25$ GeV is used to estimate the contamination of the W sample from multijet processes.

For events with an electron in the central region, the background is $3.0\% \pm 0.6\%$ (stat + syst) for $W + 0$ and $(19.3 \pm 4.3)\%$ for $W + 1$ jet events. The background for events with an electron in the forward region is $(13.3 \pm 1.6)\%$ for $W + 0$ jet and $(52.6 \pm 5.2)\%$ for $W + 1$ jet events. The uncertainties reflect systematic and statistical errors added in quadrature. The statistical uncertainty is the dominant source of error in estimating the background.

Additional sources of background to $W \rightarrow e\nu$ production are from electroweak processes which either are improperly identified in the detector or have a signature identical to that of $W \rightarrow e\nu$ production. The electroweak processes we considered are $Z \rightarrow e^+e^-$ and $q\bar{q} \rightarrow \gamma^* \rightarrow e^+e^-$ where one of the electrons is lost, and $Z \rightarrow \tau^+\tau^-$

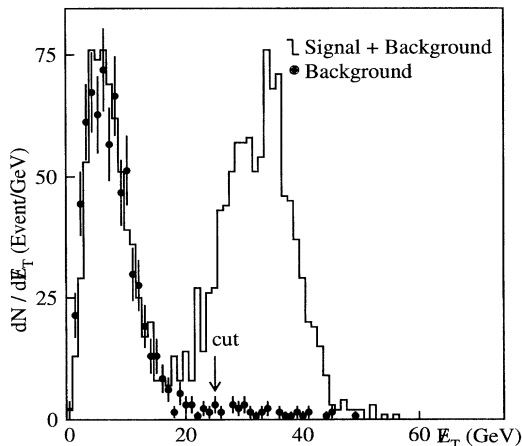


FIG. 1. \cancel{E}_T distributions for $W + 0$ jet events with the electron in the central region, $|\eta_e| < 1.2$. The histogram represents the signal plus background and solid circles indicate the background. The two distributions are normalized using the number of events in the region $\cancel{E}_T < 15$ GeV. The error bars represent statistical errors only.

where one of the τ 's decays to $e\nu\bar{\nu}$ and the other decays hadronically. We use Monte Carlo event samples to estimate the background contamination from these sources and find the level of contamination to be less than 3% of the signal for both $W + 0$ jet and $W + 1$ jet events. The process $W \rightarrow \tau\nu$ (where $\tau \rightarrow e\nu\bar{\nu}$) is considered as part of the signal because the associated jet production is independent of the W decay mode.

The number of $W + 0$ jet events, after subtracting backgrounds from multijet and electroweak processes, is 8200 ± 94 (stat) ± 61 (syst), and the number of $W + 1$ jet events is 532 ± 28 (stat) ± 49 (syst). The resulting experimental ratio of the number of $W + 1$ jet events to $W + 0$ jet events is $\mathcal{R}_{\text{exp}} = 0.065 \pm 0.003$ (stat) ± 0.007 (syst). The dominant systematic error is from the jet energy scale uncertainty. This is due to the rapidly falling shape of the jet E_T spectrum and the resulting sensitivity to the E_T^{min} cutoff. This systematic error is obtained by repeating the complete analysis, varying the jet energy scale correction within errors.

The NLO QCD predictions [3] for $W + 0$ jet and $W + 1$ jet cross sections enable parametrizations of each cross section as a power series in α_s . The theoretical predictions, using the minimal subtraction ($\overline{\text{MS}}$) scheme, take into account the effect of experimental jet energy resolution, as well as the impact of the lepton isolation criteria and other experimental constraints. The cross section for $W + n$ jets is parametrized as $\sigma_{W+n \text{ jet}} = \alpha_s^n (A_n + \alpha_s B_n)$ for $n = 0$ or 1. The coefficients A_1 and B_0 depend on E_T^{min} of the jet and B_1 depends on E_T^{min} , the choice of jet cone radius ΔR , and μ_R . The coefficients are computed for a given parton distribution function (PDF) evolved to the scale M_W . The evolution is carried out using the value for Λ_{QCD} associated with each PDF. This Λ_{QCD} value corresponds to a value of α_s , calculated at the scale M_W using the second order expression for the running coupling constant and is labeled as $\alpha_s^{\text{PDF}}(M_W)$ in Table I. The prediction for the ratio is referred to as $\mathcal{R}_{\text{pred}}$.

Figure 2 shows $\mathcal{R}_{\text{meas}}$ with its uncertainty given by the shaded area and three open symbols representing $\mathcal{R}_{\text{pred}}$ for various PDF's [11–14] at $\alpha_s = \alpha_s^{\text{PDF}}(M_W)$. The $\mathcal{R}_{\text{pred}}$ for all PDF's considered [11–15] are given in Table I. The error for each prediction reflects only the statistics used in the Monte Carlo calculation. We do not assign an uncertainty due to the choice of μ_R because the variation in the $W + 1$ jet cross section is less than 2% for $M_W/2 < \mu_R < 3M_W$ [3,16]. The dependence of $\mathcal{R}_{\text{pred}}$ and $\mathcal{R}_{\text{meas}}$ on E_T^{min} has been studied in the range $25 < E_T^{\text{min}} < 60$ GeV [5] and the relationship between data and theory does not change in this region of E_T^{min} . All theory predictions are consistent with each other and are below the data by over 1 standard deviation.

The dashed line in Fig. 2 represents the predicted ratio, as a function of α_s , for the CTEQ3M [15] parton distributions if the strong coupling constant is varied only

TABLE I. Values of α_s for various parton distributions [11–15].

PDF	$\alpha_s^{\text{PDF}}(M_W)$	$\mathcal{R}_{\text{pred}} \pm \Delta \mathcal{R}_{\text{pred}}$	$\alpha_s^{\text{ME}}(M_W) \pm \Delta \alpha_s^{\text{ME}}$
CTEQ2M	0.112	0.053 ± 0.001	0.134 ± 0.016
CTEQ2ML	0.119	0.055 ± 0.001	0.139 ± 0.017
CTEQ3M	0.114	0.053 ± 0.001	0.139 ± 0.017
MRS(D'_0)	0.113	0.056 ± 0.001	0.129 ± 0.015
MRS(D'_\perp)	0.113	0.053 ± 0.001	0.136 ± 0.016
MRS(A')	0.114	0.054 ± 0.001	0.134 ± 0.016
GRV94	0.111	0.055 ± 0.001	0.129 ± 0.015

in the hard partonic cross section (ME), leaving α_s in the parton distributions fixed at α_s^{PDF} . Lines with practically identical slopes are obtained for the other parton distributions but are not shown. The intercept of $\mathcal{R}_{\text{meas}}$ with this line yields a value of α_s (α_s^{ME}) to NLO for a particular PDF. Table I summarizes the values of α_s^{ME} , at $\mu_R = M_W$, for various PDF's along with the uncertainties. The different sources contributing to the uncertainty are summarized in Table II for the CTEQ2M parton distribution. The error $\Delta \alpha_s^{\text{ME}}$ in Table I is the quadratic sum of all these uncertainties. As expected, because all predictions are below the data, each PDF prefers a value of $\alpha_s^{\text{ME}} > \alpha_s^{\text{PDF}}$ by just over 1 standard deviation.

To determine the running coupling constant in a fully consistent manner, α_s should be varied simultaneously in both the PDF and ME. For each of CTEQ3M [11], MRS(A') [12], and GRV94 [13] distributions, we have obtained a family of new PDF's corresponding to a range

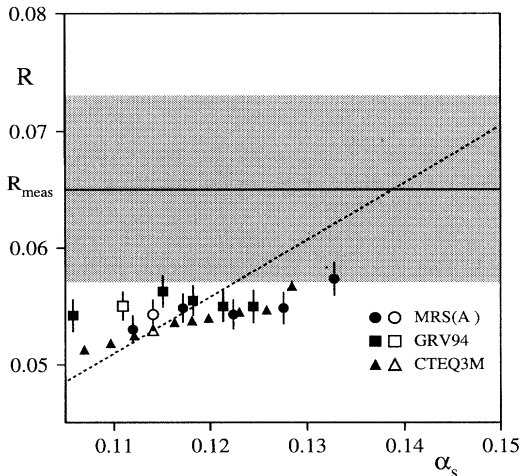


FIG. 2. \mathcal{R} vs α_s for CTEQ3M, MRS(A'), and GRV94 PDF's fitted with various values of α_s^{PDF} . The symbols represent $\mathcal{R}_{\text{pred}}$ at α_s^{PDF} for each PDF. The dashed line is the prediction for CTEQ3M PDF when α_s is varied only in the partonic cross section.

of α_s^{PDF} values, based upon the same data sets as for the standard PDF's. The family of \mathcal{R} vs α_s then calculated is shown for each PDF family as the closed symbols in Fig. 2. Statistical errors from the Monte Carlo calculation are shown for the MRS and GRV families. For the CTEQ family, the individual points are correlated due to the choice of identical random number seeds and thus have negligible relative errors. The variation of $\mathcal{R}_{\text{pred}}$ with α_s for each of these families is quite weak and remains over 1 standard deviation below $\mathcal{R}_{\text{meas}}$ for all reasonable values of α_s .

A similar study was made by the UA2 Collaboration [1] at $\sqrt{s} = 630$ GeV using $\mathcal{O}(\alpha_s^2)$ tree-level QCD calculations. Allowing α_s to vary in PDF's and ME resulted in a larger slope in \mathcal{R} vs α_s than we observe at $\sqrt{s} = 1800$ GeV. We have verified that our calculation reproduces the lower energy result and conclude that the major difference derives from the lower parton momentum fraction x values probed at the higher energy. As α_s is increased, the contribution to \mathcal{R} from the ME dependence increases but is compensated by the reduction in \mathcal{R} due to the decrease in the gluon density at the relevant x (~ 0.05) and consequent reduction in the $W + 1$ jet cross section. We conclude that the existing QCD calculations cannot be brought into agreement with the measured $\mathcal{R}_{\text{meas}}$ value, though at present the discrepancy [17] is just over 1 standard deviation.

TABLE II. Summary of uncertainties in α_s^{ME} for the CTEQ2M parton distribution.

Source	α_s^{ME}
Experimental statistics	0.005
Jet energy scale correction	0.013
Jet reconstruction efficiency	0.002
Jet energy resolution	0.005
Monte Carlo statistics	0.005
Total $\Delta \alpha_s^{\text{ME}}$	0.016

In summary, we have measured the ratio of $W + 1$ jet and $W + 0$ jet cross sections at the Fermilab Tevatron with an accuracy of about 10%. All NLO QCD predictions, using PDF's determined mainly from fits to low energy data, are below our data by over 1 standard deviation. When this measurement is used to extract a value for the strong coupling constant, we find that, after variation of α_s in PDF's is taken into account, the sensitivity to α_s is greatly reduced and an extraction of α_s is not possible.

We express our appreciation to W. T. Giele for numerous valuable discussions and for providing modifications to the theoretical predictions appropriate to this measurement. We thank the Fermilab Accelerator, Computing, and Research Divisions, and the support staffs at the collaborating institutions for their contributions to the success of this work. We also acknowledge the support of the U.S. Department of Energy, the U.S. National Science Foundation, the Commissariat à l'Énergie Atomique in France, the Ministry for Atomic Energy and the Ministry of Science and Technology Policy in Russia, CNPq in Brazil, the Departments of Atomic Energy and Science and Education in India, Colciencias in Colombia, CONACyT in Mexico, the Ministry of Education, Research Foundation and KOSEF in Korea, and the A. P. Sloan Foundation.

*Visitor from CONICET, Argentina.

†Visitor from IHEP, Beijing, China.

‡Visitor from Universidad de Buenos Aires, Argentina.

§Visitor from Univ. San Francisco de Quito, Ecuador.

- [1] UA2 Collaboration, J. Alitti *et al.*, Phys. Lett. B **263**, 563 (1991).
- [2] UA1 Collaboration, M. Lindgren *et al.*, Phys. Rev. D **45**, 3038 (1992).
- [3] W. T. Giele, E. W. N. Glover, and D. A. Kosower, Nucl. Phys. **B403**, 633 (1993).
- [4] W. T. Giele, E. W. N. Glover, and D. A. Kosower, in *Proceedings of the XXVIIth Rencontre de Moriond*, edited by J. Trân Thanh Vân (Editions Frontières, Gif-sur-Yvette, 1992).
- [5] Jaehoon Yu, Ph.D. thesis, SUNY at Stony Brook, 1993 (unpublished). This can be found on the World Wide Web (WWW) under URL : http://d0sgi0.fnal.gov/publications_talks/thesis/.
- [6] S. Abachi *et al.*, Nucl. Instrum. Methods Phys. Res., Sect. A **338**, 185 (1994).
- [7] Pseudorapidity is defined as $\eta = -\ln[\tan(\theta/2)]$, where θ is the polar angle relative to the proton beam.
- [8] M. Narain, in *Proceedings of American Physical Society Division of Particles and Fields*, edited by R. Raja and J. Yoh (World Scientific, Singapore, 1993); R. Engelman *et al.*, Nucl. Instrum. Methods Phys. Res., Sect. A **216**, 45 (1983).
- [9] A. Milder, Ph.D. thesis, University of Arizona, 1993 (unpublished). This can be found on the World Wide Web (WWW) under URL : http://d0sgi0.fnal.gov/publications_talks/thesis/.
- [10] H. Weerts, in *Proceedings of the 9th Topical Workshop on Proton-Antiproton Collider Physics*, edited by K. Kondo and S. Kim (Universal Academy Press, Tokyo, 1994).
- [11] W. K. Tung and H. L. Lai (private communication).
- [12] A. D. Martin, W. J. Stirling, and R. G. Roberts Durham Report No. DTP/95/48, 1995 (to be published).
- [13] A. Vogt, Report No. DESY 95-068, (to be published).
- [14] CTEQ Collaboration, H. L. Lai *et al.*, Phys. Rev. D **51**, 4763 (1995).
- [15] A. D. Martin, R. G. Roberts, and W. J. Stirling, Phys. Lett. B **306**, 145 (1993); **309**, 492 (1993).
- [16] W. T. Giele (private communication).
- [17] NLO jets have more fractional energy in a cone of 0.7 than data jets [18]. Therefore, a mismatch in energy between theory and data jets increases the discrepancy in \mathcal{R} by an estimated amount of 0.005/GeV.
- [18] S. Abachi *et al.*, "Transverse Energy Distributions within Jets in $\bar{p}p$ Collisions at $\sqrt{s} = 1.8$ TeV," Phys. Lett. B (to be published).